Environmental Science: Atmospheres

ROYAL SOCIETY OF CHEMISTRY

PAPER

View Article Online
View Journal | View Issue

Cite this: *Environ. Sci.: Atmos.*, 2023, **3**, 408

Estimations of NO_x emissions, NO_2 lifetime and their temporal variation over three British urbanised regions in 2019 using TROPOMI NO_2 observations†

Matthieu Pommier

Quantification of air pollutant emissions is crucial to accurately model their concentrations. Nitrogen oxides (NO_x: nitrogen dioxide NO_2 and nitric oxide NO) have adverse effects on health, agriculture and natural ecosystems both directly and due to their role in the formation of secondary pollutants. This work estimates annual total NO_x emissions, mean NO_2 lifetime, their seasonal variation and the weekday–weekend effect, over three selected British urban areas with NO_2 pollution (London, Manchester and Birmingham). The method combines an exponentially modified Gaussian fitting function and wind rotation technique, using TROPOMI tropospheric NO_2 observations together with reanalysis wind fields. The analysis for 2019 yields total emissions of 113 kT of NO_x over London, and 37 kT and 22 kT over Manchester and Birmingham, respectively. Compared to the UK National Atmospheric Emissions Inventory, this represents an increase of 6% for Manchester, 18% for London, and a decrease of 33% for Birmingham. These values are improved compared to a recent published study finding larger discrepancies with the same inventory (from 55% to 105% for the relevant cities), despite some overall consistencies. The weekday NO_x emissions are larger than at the weekend, by a factor of 1.54 for Manchester, 2.68 for London and 3.05 for Birmingham. Notably, it has been found Birmingham has a longer NO_2 mean lifetime for weekdays (~6 h) than for the weekends (~2 h) and Manchester presents a mean NO_2 lifetime almost 4 times higher in summer (6.13 h) than in autumn (1.64 h). More generally, the findings on emission, emission rate and lifetime suggest management of emissions might be needed for weekdays in London and Birmingham, and for weekends in Manchester.

Received 12th July 2022
Accepted 16th December 2022

DOI: 10.1039/d2ea00086e

rsc.li/esatmospheres

Environmental significance

The quantification of nitrogen dioxide (NO_2) concentrations, a major contributor to poor air quality in urban areas, using atmospheric models relies on accurate quantification and spatial representation of the sources and their emissions. This study estimates annual total nitrogen oxide (NO_x: consisting of NO_2 and nitric oxide, NO) emissions and mean NO_2 lifetimes using satellite observations combined with reanalysis wind fields, over three British urban areas with exceedances of NO_2 standards, *i.e.* London, Manchester and Birmingham. The results are compared with emission mass estimates from the UK National Atmospheric Emissions Inventory and discussed alongside estimates in the literature. The temporal variation is estimated, focusing on the weekday–weekend effect and seasonal variation suggesting different emission management strategies in the studied cities.

1. Introduction

Nitrogen oxides (NO_x), consisting of nitrogen dioxide (NO_2) and nitric oxide (NO), are important atmospheric trace gases that actively participate in the formation of tropospheric ozone and secondary aerosols and accordingly have a significant effect on human health and the climate.[1,2] NO_x can be emitted by natural sources such as lightning, microbial processes in soils and naturally occurring wildfires but anthropogenic activities represent the major contributor in the UK.[3] Fossil-fuel burning from mobile and industrial emitters represents the largest source of anthropogenic NO_x emissions. These sources are usually clustered near densely populated urban areas.[4]

Since NO_x is a short-lived gas in the atmosphere with a lifetime of several hours, especially in the boundary layer during the daytime,[5,6] strong spatial gradients in the geographical distribution can be observed. This results in some large NO_2 hotspots over urbanised areas which can be observed from space.[7,8]

These observations from space are becoming more accurate thanks to the new generation of atmospheric sounders such as

Ricardo Energy & Environment, 18 Blythswood Square, Glasgow G2 4BG, UK. E-mail: matthieu.pommier@ricardo.com

† Electronic supplementary information (ESI) available. See DOI: https://doi.org/10.1039/d2ea00086e

the TROPOspheric Monitoring Instrument (TROPOMI)[9] which has a spatial resolution about 16 times better than its predecessor (the Ozone Monitoring Instrument – OMI[10]).

Despite this progress, the estimates of NO_x emissions in emission inventories are still uncertain. The knowledge of the emissions is crucial to better model the NO_2 concentrations and thus to be able to produce relevant strategies to reduce air pollution. This issue is pertinent to the World Health Organization (WHO), which has issued new guideline air quality levels to protect the health of populations.[11] The new guideline level for NO_2, which is 10 μg m^{-3} as an annual average, corresponds to a reduction of 30 μg m^{-3} from the previous WHO guideline (issued in 2005). In the UK, 33 zones out of 43 exceeded the 40 μg m^{-3} annual limit of NO_2 concentrations in 2019,[12] which highlights the scale of the challenge faced by all European governments in meeting the new annual limit.

The estimation of anthropogenic NO_x emissions for a region traditionally relies on a "bottom-up" method that is based on the quantification of total fuel use coupled with averaged emission factors for different emitting sectors, technologies and processes. Hence, they are subject to uncertainties due to an incomplete understanding of sectoral activity, real-world operating conditions and spatial distributions of sources. Additionally, estimates of NO_x emissions may become outdated when fuel consumption and emission factors change. This commonly happens during emission inventory compilation cycles, the methods and data sources for which evolve and improve over time. The hosting of a worldwide event such as the Olympic Games in London in 2012 or more recently, the exceptional situation of the COVID-19 pandemic in 2020, are good illustrations of sudden changes in our NO_x emitting activities (*e.g.* industrial processes and road transport) which are not well represented in emission inventories. The satellite instruments can therefore act as key observers of these changes and the data collected can allow quantification of the changes in emissions[13] that are overlooked by standard inventories.

"Top-down" emission estimates can be made by assimilating observations, such as those from satellite instruments, into a chemical-transport model (CTM). However, this method involves complex and computationally expensive inversion algorithms.[14] The accuracy of these estimated emissions also relies on the models' capability to correctly represent the chemistry and thus pollutants' concentrations, which can sometimes involve complex chemical regimes and is subject to uncertainty. This is particularly apparent in an urban environment which is impacted by several major source sectors, each with complicated temporal, physical and spatial characteristics that influence their effect on concentrations.

During the last decade, some less sophisticated methods to derive emissions from satellite observations without the use of CTMs have started to emerge.[5] For example, the method presented in Beirle *et al.* (2011),[5] based on exponential-modified Gaussian (EMG) plume fit, infers the NO_x emissions from NO_2 observed from space, in air advected over the source regions. This method also considers the influence of wind speed and wind direction on concentrations. Binning the data by wind direction allows simultaneous estimates of both emission strengths and atmospheric residence times. According to Lorente *et al.* (2019),[15] under non-stagnant conditions, the chemical decay of NO_2 in the boundary layer is of minor importance in average concentrations given the short time required for the pollutant to travel through the source region such as a city. The EMG fit has been shown to provide the best estimates, compared with other fitting functions, in emissions and species lifetime across the range of several wind conditions and across the different chemical cases.[16]

This study aims to estimate the NO_x emissions based on NO_2 observations provided by TROPOMI. The work has focused on three large British cities: London, Manchester and Birmingham. While Pope *et al.* (2022)[17] adapted the technique of Beirle *et al.* (2011)[5] to estimate the NO_x emissions in some UK cities, this work combines EMG with a wind rotation technique[18,19] to calculate NO_x emissions with a similar method used by Fioletov *et al.* (2015)[20] for SO_2. The rotation technique, where each pixel is rotated around the point source according to the wind direction so that all pixels appear to have the same wind direction, accumulates a statistically significant data set.

The method presented in this study provides a unique emission estimate irrespective of the wind direction over the selected source regions unlike the estimates of Beirle *et al.* (2011)[5] or those for the UK by Pope *et al.* (2022).[17] It also allows the use of a distinct calendar year of observation while Pope *et al.* (2022)[17] needed to gather the observations during a longer period (Feb 2018–Jan 2020) to compare to a distinct National Atmospheric Emission Inventory (NAEI) reported year. The NO_x emissions are calculated herein for the year 2019 and are compared to the recently reported UK NAEI.[21] 2019 has been selected since it represents a typical year, not influenced by exceptional conditions in emissions (*e.g.* lockdowns in 2020) and in meteorology, since 2019 was not a stormier year compared to recent decades[22] and the wind data are crucial in the method. The data used in this work are described in Section 2 and the Methods in Section 3. The comparison between the satellite-based estimates and the NAEI, and then with previous estimates given by Pope *et al.* (2022)[17] is presented in Section 4 "Results". The results also show the weekday–weekend and seasonal NO_x emissions and the corresponding mean NO_2 lifetime. The conclusions are given in Section 5.

2. Data used

2.1 TROPOMI

The satellite-based NO_2 tropospheric columns from TROPOMI (TROPOspheric Monitoring Instrument) have been used to derive the NO_x emissions. TROPOMI was launched on 13 October 2017 by the European Space Agency (ESA) for the European Union's Copernicus Sentinel-5 Precursor (S-5P) satellite mission. The satellite follows a sun-synchronous, low-

earth orbit (at 825 km of altitude) with an equator crossing time near 13:30 local solar time. This corresponds to an overpass time over the UK between approximately 11:00 and 14:00 UTC.

TROPOMI measures atmospheric column amounts of several trace gases in the UV-vis-near infrared-shortwave infrared spectral regions. At the nadir, pixel sizes are 3.5 km × 7.2 km with little variation in pixel sizes across the 2600 km swath. In August 2019, the pixel size was reduced further to 3.5 km × 5.5 km by reducing along-track averaging. One orbit around the Earth takes about 100 minutes, which, in combination with the wide swath, provides daily global coverage.

In this study, offline TROPOMI tropospheric NO_2 data with quality assurance values larger than 0.75 have been used. This criterion removes cloud-covered scenes, partially snow/ice-covered scenes, errors and problematic retrievals, as recommended by respective technical descriptions‡. This dataset is freely available at **https://s5phub.copernicus.eu/**. It is important to know that validation studies have shown that TROPOMI tropospheric NO_2 columns are biased low by about 30–50%, mainly for polluted conditions, while this bias decreases for scenes with lower NO_2 (*e.g.* Verhoelst *et al.*, 2021).[23] The causes of this bias are multiple and can be related to a misrepresentation of the aerosol opacity, an incorrect *a priori* NO_2 profile, an incorrect treatment of cloud properties, *etc.*

In this work, it is assumed that the impact of the diurnal variation of the emissions on the NO_2 tropospheric columns measured by TROPOMI remains limited, unlike the impact of the diurnal variation on surface measurements as explained by Fioletov *et al.* (2022).[13] Some ground-based measurements of the tropospheric NO_2 column have shown hourly variability depending on the location.[24,25] However, it is a fair assumption to state that the overpass time of the satellite captures the daily NO_2 tropospheric mean value, especially as the boundary layer is well mixed at this time.[8,15]

2.2 Meteorological data: wind and boundary layer height

In addition to the TROPOMI tropospheric NO_2 data, wind speed and direction are required for this work. The wind data are provided by the European Centre for Medium-Range Weather Forecast (ECMWF), ERA5 reanalysis hourly data with a horizontal resolution of 0.25° × 0.25°.[26] These wind fields are collocated in space and time to the TROPOMI observations. Thus, only the closest wind field in time and space has been used in this work and the temporal variations in wind fields as done in Liu *et al.* (2022)[27] have not been investigated.

Since most of the NO_2 is emitted within the boundary layer, the study has been refined by also using the planetary boundary layer height (PBLH) from ERA5 reanalysis hourly data. This data set has also been collocated in space and time to the TROPOMI observations. Indeed, it has been calculated that between 93 and 94% of the annual mean 1000–500 hPa NO_2 in 2019 are located below 900 hPa by using the data from the Copernicus Atmosphere Monitoring Service (CAMS) EAC4 global reanalysis§ over the three studied domains. These domains are explained in Section 3.2.2.

The value of 900 hPa corresponds to the calculated mean PBLH with the ERA5 data, associated with the satellite pixels over the three urbanised areas studied in this work (903 hPa in London, 915 hPa in Manchester and 909 hPa in Birmingham). Thus, the vertically integrated wind data between pressure levels 1000 and 900 hPa have been used to calculate the emissions and lifetimes. A sensitivity test has also been performed by using the pressure levels from 1000 to 925 hPa, and from 1000 to 875 hPa. The use of these vertically integrated wind data within the PBL, instead of using a single level, has also the advantage of limiting the impact of seasonal variability of the wind in the PBL.

Only the pixels with associated wind speeds from 1 to 50 km h^{-1} have been used for the calculation of the NO_x emissions and lifetimes. This avoids abnormally high concentrations under stagnant conditions and extremely low values under highly disturbed conditions. This selection also allows a stable fit for these calculations. The details on the fitting procedure and NO_x estimates are given in Section 3.2.

2.3 NAEI

To assess the annual NO_x emissions calculated in this study, NAEI which is the official "bottom-up" inventory of primary sources of emissions in the UK has been used. NAEI is compiled on an annual basis according to internationally agreed methodologies,[28] and updated every year by Ricardo Energy and Environment on behalf of the UK Government. NAEI provides estimates of the annual mass of total UK emissions, split by sector. It provides maps of UK emissions at 1 km × 1 km resolution for each of the 11 United Nations Economic Commission for Europe (UNECE) source sectors using the Selected Nomenclature for reporting of Air Pollutants (SNAP) and to the Gridded Nomenclature for Reporting (GNFR) sectors for international reporting. The 2019 NO_x NAEI emissions have been used for comparison with the TROPOMI-based NO_x emissions, even if it is worth knowing that only anthropogenic emissions are referenced in the NAEI while the TROPOMI-based NO_x emissions do not distinguish the natural and anthropogenic sources.

3. Methods

3.1 NO_2 high-resolution maps

To map the NO_2 distribution at high resolution and highlight the regions with the larger columns, the approach developed by Fioletov *et al.* (2011)[29] has been applied. This approach slices each satellite pixel into multiple sub-pixels, which are mapped onto a high-resolution grid. With this technique, the average of all satellite pixels centred within a several kilometres radius

‡ **https://sentinels.copernicus.eu/web/sentinel/technical-guides/sentinel-5p/products-algorithms**

§ EAC4: **https://ads.atmosphere.copernicus.eu/cdsapp#!/dataset/cams-global-reanalysis-eac4?tab=form**

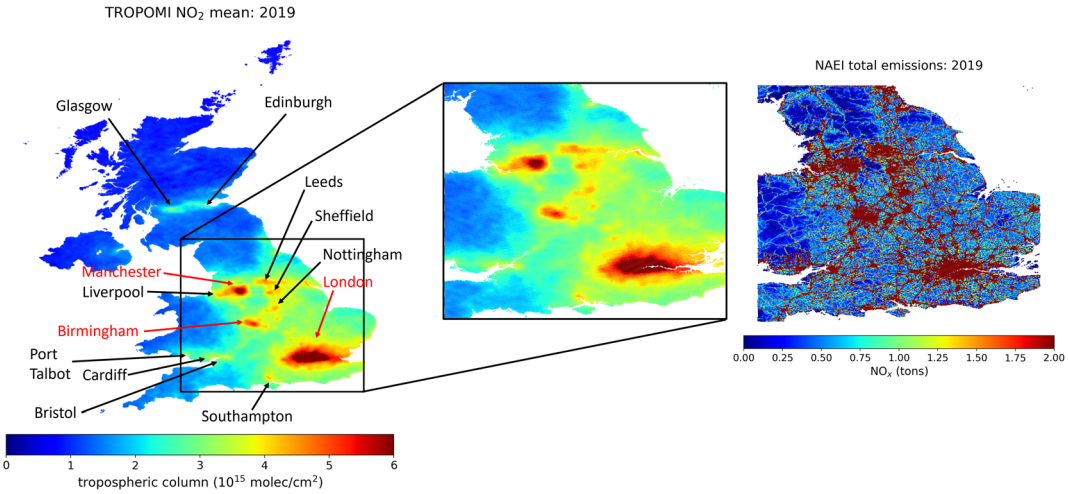

Fig. 1 Mean TROPOMI NO_2 tropospheric column over the UK in 2019 at 1 km × 1 km resolution. A zoom over the part of the map highlighted by a black box is presented and as a comparison, the total NAEI NO_x emissions in 2019 are shown for the same zone. Only the pixels over land are plotted, so the NAEI NO_x shipping emissions are not shown. The cities written in red correspond to the studied urbanised areas. Other cities are listed as an indication.

from each grid point is calculated. In our case, a radius of 5 km has been used. This approach exploits the large number of TROPOMI observations gathered during a selected period and helps to artificially increase the resolution of the spatial distribution. The horizontal resolution of 1 km × 1 km (comparable to the NAEI resolution) has been used. Both spatial distributions, *i.e.* from the satellite observations and NAEI, have been calculated on the WGS84 projection (Fig. 1). In this way, the NO_2 distribution is aligned to the NAEI grid cells which allows for the comparison.

Fig. 1 clearly shows large NO_2 hotspots over the main urbanised areas in the UK, such as London, Birmingham and Manchester. In addition, other locations can be distinguished such as Glasgow, Edinburgh and Southampton. This matches the larger NO_x emission regions referenced in the NAEI even if some discrepancies can be noted. For example, the main roads are not easily identified in the TROPOMI NO_2 distribution map, but we can see the belt drawn by cities such as Leeds, Sheffield and Nottingham and the one between Bristol, Cardiff and Port Talbot. Other cities such as Liverpool are also more difficult to identify due to the influence on the map symbology from the presence of a larger amount of NO_2 in other cities, such as Manchester.

3.2 NO_x emission estimates

3.2.1 Rotation technique. For the emission estimation, the wind rotation technique has been applied. This technique was introduced by Valin *et al.* (2013),[19] whereby each observation is rotated around the presumed point source according to the horizontal wind direction so that all observations appear to have the same wind direction. This wind-rotation technique is further explained in Pommier *et al.* (2013)[18] and used by Fioletov *et al.* (2015)[20] to estimate emissions.

The common upwind-to-downwind wind direction has been defined in the North–South direction. The alignment in a common upwind-to-downwind direction increases the number of observations used for analysis without introducing additional errors for point sources, compared with individually analysing observations using wind directions.[27] This statistically significant data set allows calculating a unique emission estimate irrespective of the wind direction unlike the estimates given by Pope *et al.* (2022).[17] The rotation technique also allows splitting the background and enhanced conditions.

However, for sources located in an area with multiple surrounding sources, the rotation technique may result in significant bias. This might allocate the NO_2 from interfering sources into a ring of elevated NO_2 values around the source of interest and thus wrongly amplifying the NO_2 signal of the studied source.[20,27] To limit this problem, the intervals used for the fit are adapted to the size of the selected urbanised area. These intervals are given in the following Section 3.2.2.

3.2.2 Exponentially modified Gaussian fitting procedure. While Beirle *et al.* (2011)[5] introduced the EMG fitting procedure to derive NO_x emissions without the use of a CTM, Fioletov *et al.* (2015)[20] and de Foy *et al.* (2015)[30] advanced this even further by employing the plume rotation technique to quantify emissions from isolated US power plants and cities.

The EMG method allows estimating the lifetime ($\tau = 1/\lambda$, with λ being the NO_2 decay rate), the plume spread (σ), the emission enhancement (A) of the point source (in our case a whole urbanised area) and a background (B) if it is applied.

De Foy *et al.* (2014)[16] showed that the EMG fitting function provides accurate estimates of emissions and species lifetime across the range of several wind conditions and across different chemical cases. Despite its good performance, it is important to note this method is sensitive to the wind fields (direction and speed) used and does not describe the full chemistry in the plumes as would be calculated in a CTM. The estimates can also be impacted by the accuracy of the location of the sources and

thus by the coordinates used to define the centre of this location.

In this work, the EMG method has been applied and defined as a two-dimensional function, following eqn (1) hereafter:

$$\text{fit NO}_2\ (x,y,s) = A\text{f}(x,y)\text{g}(y,s) + B \quad (1)$$

where the fit NO_2 is the product of a Gaussian function f(x,y), given in eqn (2) and the exponentially modified Gaussian function g(y,s), given in eqn (3), taking into account B, the background NO_2 (tropospheric column in molecules per cm^2) and the emission enhancement A (in molecules per cm^2).

$$\text{f}(x,y) = \frac{1}{\sigma_1\sqrt{2\pi}}\exp\left(\frac{x^2}{2{\sigma_1}^2}\right) \quad (2)$$

$$\text{g}(y,s) = \frac{\lambda_1}{2}\exp\left(\frac{\lambda_1(\lambda_1\sigma^2+2y)}{2}\right)\text{erfc}\left(\frac{\lambda_1\sigma^2+y}{\sqrt{2}\sigma}\right) \quad (3)$$

x and y (in km) correspond to the coordinates of the rotated TROPOMI pixel center, s is the allocated wind speed (in km h^{-1}) and $\text{erfc}(x) = \left(\frac{2}{\sqrt{\pi}}\int_{\pi}^{\infty}\exp(-t^2)\text{d}t\right)$ is the Gauss error function.

Eqn (2), f(x,y), describes the diffusion of NO_2 perpendicular to the downwind direction. Eqn (3), g(y,s), describes the diffusion (with the plume spread σ) that smooths an exponential function, giving the exponential decay of the NO_2 in the downwind direction. The use of σ_1 that increases with the distance from the source instead of σ in f(x,y) aims to reflect the change in the winds between the source and the analysed pixel that yields an additional spread of the "plume" after the rotation of all pixels in a upwind–downwind direction, as detailed in Fioletov *et al.* (2015)[20] and used in Dammers *et al.* (2019).[31] The σ_1 is described in eqn (4).

$$\sigma_1 = \begin{cases} \sqrt{\sigma^2 - 1.5y}, & y<0 \\ \sigma, & y>0 \end{cases} \quad (4)$$

And λ_1 is the ratio of the decay rate to the wind speed:

$$\lambda_1 = \frac{\lambda}{s} \quad (5)$$

The fits have been performed in Python using the non-linear curve fit package from the SciPy module[32] using the Levenberg–Marquardt algorithm, which minimizes the difference between the given distribution and the fitted values. The fitting was done for a ±50 km area from the centre of London and ±30 km from the centre of Manchester and Birmingham.

The NO_2 emission rate E (in molecules per cm^2 per h) is given by eqn (6):

$$E = A \times \lambda \quad (6)$$

To then derive the NO_x emissions (E_{NO_x}), we use the following eqn (7):

$$E_{\text{NOx}} = 1.32 \times E \quad (7)$$

The value of 1.32 is used to scale the NO_2 emissions to derive the NO_x emissions. It is based on the NO_x/NO_2 concentration ratio representing the "typical urban conditions and noontime sun"[1] and is commonly used for the calculation of the NO_x estimates.[5,17,33] It is worth noting that Goldberg *et al.* (2019)[34] used a ratio of 1.33 for their study in North America while Verstraeten *et al.* (2018)[35] used a ratio calculated by a regional chemical-transport model and Lange *et al.* (2022)[8] directly converted the NO_2 columns for each pixel into NO_x columns, assuming that the Leighton photostationary state applies for the polluted air masses investigated. This conversion from NO_2 to NO_x has not been investigated in this study.

The selection of the input parameters used in the fitting procedure has been based on an initial assessment of the studied sources (*e.g.* for the plume spread) and an initial fit at different wind speeds (*e.g.* for the lifetime).[20,31]

The recent work done by Fioletov *et al.* (2022)[13] added a more sophisticated background offset than the one used in this work. Their background is linked to the elevation, depending on the geographical coordinates. A variable background offset has also been applied in Beirle *et al.* (2019).[36] Beirle *et al.* (2019)[36] subtracted the 5th percentile of all tropospheric columns within their considered regions. The variability of this background has not been tested in this study and it is assumed to remain limited thanks to the estimation of this background during the fitting procedure, especially with the upwind data, as done by previous studies.[8]

3.2.3 Selection of the studied cities. It has been recognized the method better suits sources with high contrast between source and background,[8,13] so the method has been tested over other locations. Regions less affected by clouds should also be preferred to maximize the number of satellite observations which can be used.

To characterize the NO_2 signature over these three cities, a signal-to-noise ratio (SNR) test has been performed following a similar concept to the technique described in McLinden *et al.* (2016).[37] This SNR helps to inform on the conditions suitable for our calculations. The SNR has been calculated following eqn (8).

$$\text{SNR} = \frac{c_\text{d} - c_\text{u}}{\frac{\sigma_\text{d}}{\sqrt{N_\text{d}}} - \frac{\sigma_\text{u}}{\sqrt{N_\text{u}}}} \quad (8)$$

where c_d and c_u are the mean downwind and upwind tropospheric columns calculated in the areas shown in Fig. S1.† σ_d and σ_u are the corresponding standard deviations and, N_d and N_u are the number of observations.

A summary of the SNR tested over different locations is presented in Table S1.† This shows that only the three studied cities, among those tested, have a large annual SNR (>8). This suggests some parts of the UK won't meet the requirement for inventory checking with this method. This also shows the calculation of these emissions for future years might be more challenging in case the emissions dramatically decrease and these SNRs are reduced. This in turn also means that the method may be difficult to apply in cities where the SNR is too low, perhaps due to the confounding effect of typically cloudy conditions and comparatively low NO_2 tropospheric columns, for example in Cardiff and Swansea.

4. Results

4.1 Annual NO_x emissions and mean NO_2 lifetime

As explained in Section 2.2, the mean PBLH over the 3 studied urban areas is close to 900 hPa. Thus, the calculation of the emissions and lifetimes have been based on the vertically integrated wind data between pressure levels 1000 and 900 hPa. For comparison, the NAEI total NO_x emissions have been used and integrated in the same area as the calculated estimates, *i.e.* in a region of ±50 km from the centre of London, and ±30 km from the centre of Manchester and Birmingham.

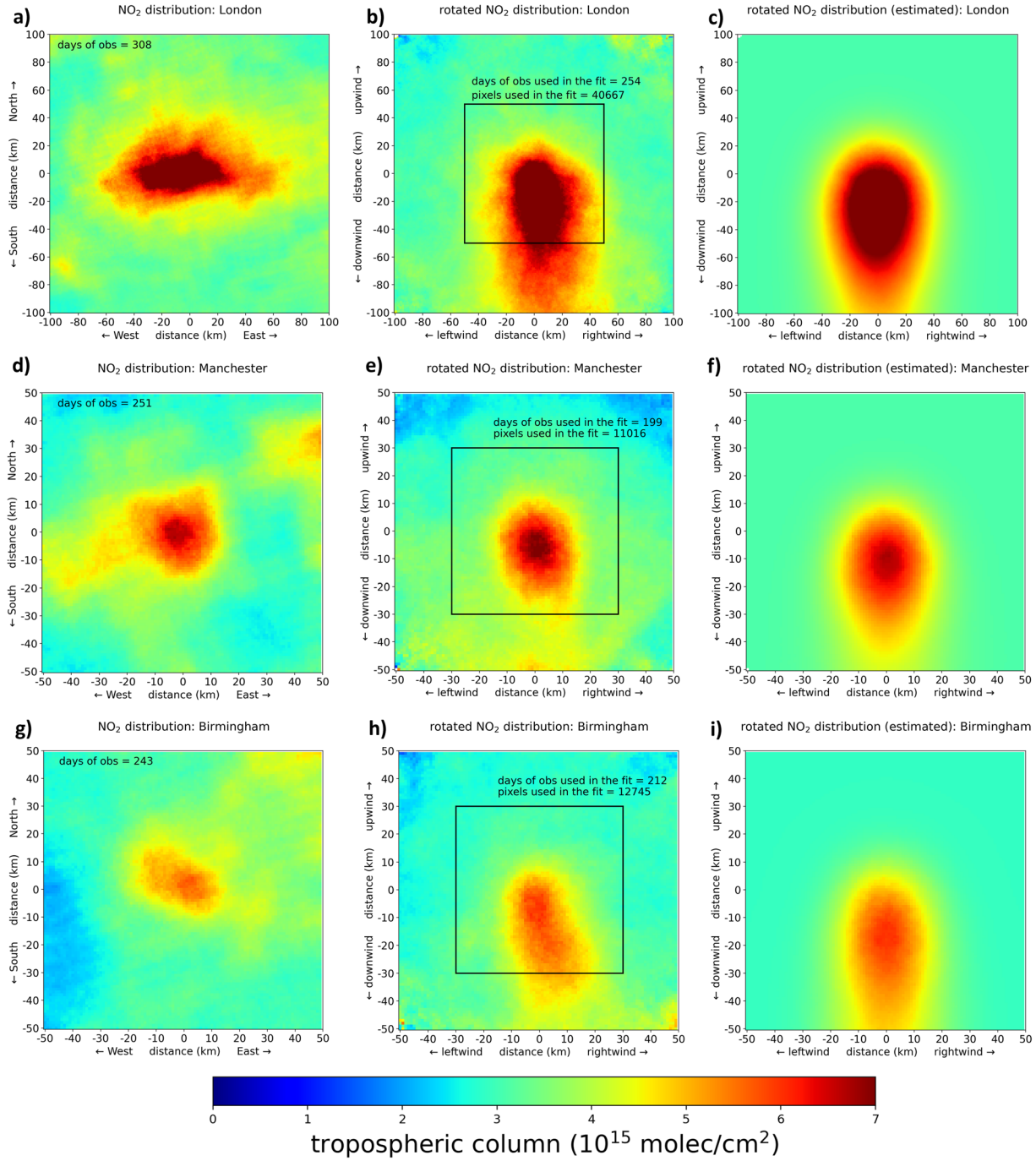

Fig. 2 NO_2 tropospheric column observed in 2019 (a, d and g), rotated around the centre of the map (b, e and h) and fitted (c, f and i) at 1 km × 1 km resolution, over London (top panels), Manchester (middle panels) and Birmingham (bottom panels). While all the *x* and *y* axes refer to the distance from the centre of the map (0,0), the axis in map (a) refers to the North/South and West/East directions, and the axis in maps (b) and (c) refers to the upwind/downwind and left-wind/right-wind directions. As an illustration, the black box in map (b, e and h) corresponds to the ±50 km (London) or ±30 km (Manchester and Birmingham) area used by the fitting function and for the calculation of the emission rate and lifetime. The number of days of observations over the plotted domain for the three studied areas is given (a, d and g), and the number of days of observations and number of pixels within the black box and used for the fit are also provided (b, e and h).

Fig. 2 illustrates the fitting procedure by showing NO_2 distribution over London, Manchester, and Birmingham at 1 km × 1 km resolution in 2019 (panels a, d and g), the redistributed NO_2 in a common upwind-to-downwind manner as explained in Section 3.2.1 (panels b, e and h) and the fitted upwind-to-downwind distribution (panels c, f and i). It is clear that London, with its larger conurbation, has a wider spatial spread in the NO_2 distribution, which has been already seen in Fig. 1. Fig. 2 also shows the impact of the wind direction in the NO_2 distribution, especially in London and Birmingham (Fig. 2b and h) and the fitting procedure tends to fairly reproduce the idealised situation (Fig. 2c, f and i).

Fig. 3 shows the zonally integrated NO_2 tropospheric columns for the three studied areas after rotation of all pixels in an upwind–downwind direction, with the corresponding fitted emission rate (converted into NO_x in Mg h^{-1}) and mean NO_2 lifetime. Fig. 3 highlights the downwind spread of the NO_2 from the source location. The upwind NO_2 tropospheric column values can be interpreted as the background distribution.

The estimates rely on the wind information in the PBL, and other pressure levels have also been used. To ensure the robustness of these estimations, the same calculations have also been performed by using the pressure levels from 1000 to 925 hPa, and from 1000 to 875 hPa. This results in a standard deviation of the estimates. Fig. 3 shows that the mean NO_x emission rate is larger in London (close to 13 Mg h^{-1} ± 0.74) than in Manchester (~4.2 Mg h^{-1} ± 0.04) and Birmingham (~2.5 Mg h^{-1} ± 0.3).

The plume spread (σ) (not shown) is almost twice larger in London (23.3 km ± 0.26) than in Manchester and Birmingham (11.3 ± 0.20 and 11.7 ± 0.74, respectively).

While the mean wind speed is similar in these three large conurbation areas (~24 km h^{-1}), the NO_2 lifetime is shorter in Manchester (~1.6 h ± 0.02) and larger in Birmingham (~6 h ± 0.65). Interestingly, there is no clear difference in the meteorological conditions for both areas, *i.e.* similar total precipitation, mean temperature at 2 m, and surface net solar radiation using the CAMS ECA4 data (not shown). Valin *et al.* (2011)[38] showed that the NO_2 lifetime depends on the NO_2 and OH columns; however, the mean tropospheric column is similar in Manchester (4×10^{15} molecules per cm^2) than in Birmingham (3.8×10^{15} molecules per cm^2). This might suggest a different regime in both cities. In London, the estimated lifetime is close to 3 h.

For comparison, the NO_x emission rate for London corresponds to a similar value to a city such as Toronto, and half of New York city's value.[34] However, it is important to know that these North American values do not correspond either to the same period (5 months *vs.* full year) or the same year (2018 *vs.* 2019). In addition, the emission rate calculated in the large area including Birmingham is close to the value found for a single coal power station in South Africa[39] (Matimba power station and Majuba power station with 0.67 kg s^{-1} each, *i.e.* ~2.4 Mg h^{-1}). However, as for the study done by Goldberg *et al.* (2019),[34] the dataset used in Beirle *et al.* (2021)[39] also does not cover the same period than this work (~2 years, from Jan 2018 to Dec 2019 *vs.* 2019 in this work).

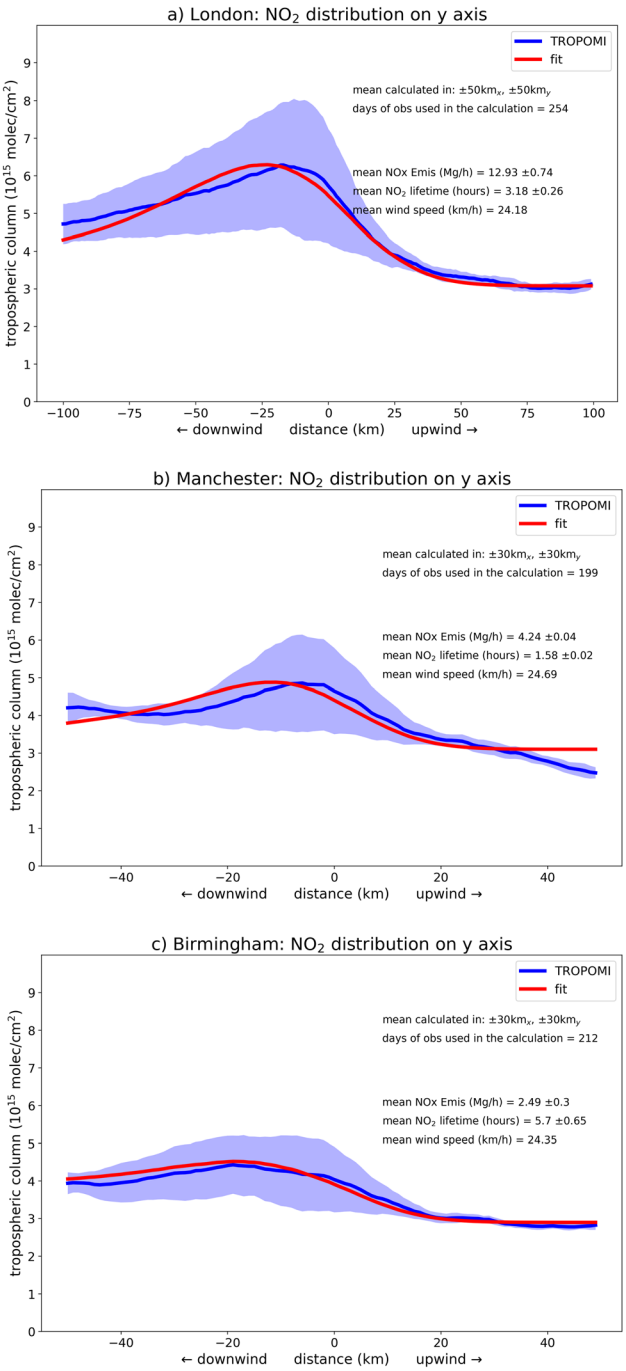

Fig. 3 Zonally integrated TROPOMI NO_2 tropospheric column (±50 km on the *x*-axis for London (a), ±30 km Manchester (b) and Birmingham (c)) (blue) after rotation of all pixels in an upwind–downwind direction and the corresponding fitted values (red) along the *y*-axis. The shade blue colour corresponds to the standard deviation in the integrated zone. The centre of the studied source is located at the point "distance 0". The mean NO_x emission rate, mean NO_2 lifetime and mean wind speed within the domain highlighted by the black box in Fig. 2 are also provided. The standard deviation of the NO_x emission rate and NO_2 lifetime is calculated using also the estimates based on vertically integrated wind fields between 1000 and 925 hPa, and between 1000 and 875 hPa.

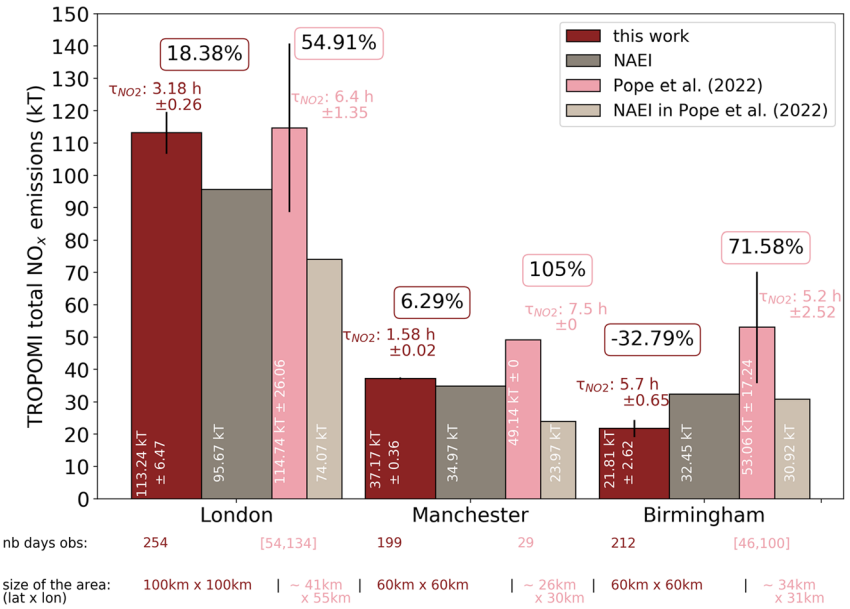

Fig. 4 Bar plot showing the TROPOMI NO_x emission (in kT) calculated in this work (burgundy) and the corresponding NAEI NO_x emission (brown) in 2019 for London, Manchester and Birmingham. The values are also given in white in each bar. The mean TROPOMI NO_2 lifetime is also provided. The calculation is based on the vertically integrated 1000–900 hPa wind field. The standard deviation of the TROPOMI NO_x emission and NO_2 lifetime is calculated in this work with also the estimates using the vertically integrated wind field between 1000 and 925 hPa, and between 1000 and 875 hPa. The relative difference in percent between the TROPOMI NO_x emissions and the NAEI NO_x emissions is given and highlighted in a colour frame. For comparison, the TROPOMI NO_x emission (in kT) calculated in Pope *et al.* (2022)[17] (pink) and their corresponding NAEI emission (light brown) are also shown. Their standard deviation is the result of the variation of their estimates depending on the wind direction. The number of days of observations used for each mean estimate is provided below with the corresponding colour. The interval of numbers is due to the variation in the number of days used in Pope *et al.* (2022).[17] The size of each urban area used in this study and in Pope *et al.* (2022)[17] is also provided below.

By assuming that the calculated emission rates are constant throughout the year, this results in a NO_x emission value of 113 kT (±6.5), 37 kT (±0.4) and 22 kT (±2.6) in 2019 for London, Manchester and Birmingham, respectively (Fig. 4). This represents an increase of 6% and 18% compared to the NAEI for Manchester and London, respectively (Fig. 4). The calculated value is about 33% lower than the NAEI for the area over Birmingham.

4.2 Comparison with Pope *et al.* (2022)[17] estimates

In this section, a comparison of the TROPOMI-based estimates with the values given in Pope *et al.* (2022)[17] for the same regions is performed. It is worth restating that the values calculated by Pope *et al.* (2022)[17] do not correspond to the same period (Feb 2018–Jan 2020 *vs.* 2019 in this study) and the areas represented in their work are smaller than the areas covered in this study (100 km × 100 km for London and 60 km × 60 km for Manchester and Birmingham). The areas used in Pope *et al.* (2022)[17] have been calculated with the NHC-NOAA converter¶ based on the coordinates given in their study. The difference in the size of the studied area can be seen with their different NAEI NO_x emission compared to NAEI emissions presented in this work (Fig. 4). However, it remains unclear how the NAEI values given in Pope *et al.* (2022)[17] were calculated. They provided the NAEI emission rate (in mol s^{-1}) which has been converted here into emissions in kT for comparison (*e.g.* 30.90 mol s^{-1} in London is equivalent to 74.07 kT, while the NAEI 2019 NO_x emissions for their area – 51.32–51.69° N, 0.52° W–0.28° E – should be around 47 kT).

Moreover, the calculation done in Manchester by Pope *et al.* (2022)[17] is only based on 29 exploitable days of observation, between 46 and 100 for Birmingham and between 54 and 134 for London, despite the large period of observations used (~2 years).

It should be noted that their estimates have a large variability, for example, their NO_x emission rate for London varies from 32.5 to 55.90 mol s^{-1} (78 and 134 kT, respectively), depending on the selected wind direction.

In addition, Pope *et al.* (2022)[17] decided to filter out small negative tropospheric columns (>-1×10^{-5} mol m^{-2}) which might introduce an artificial positive bias in their average. On the opposite, they used a stringent criterion on the wind speed (>2 m s^{-1}) which might lead to an underestimation of their NO_x emissions. They also only used the wind data at 13:00 UTC in their calculation which does not always represent the best time collocation with the satellite overpass.

These differences can explain the differences found between the NO_x emissions estimated in this study and theirs (Fig. 4), especially in Manchester and Birmingham. Surprisingly,

¶ https://www.nhc.noaa.gov/gccalc.shtml

Table 1 Relative difference (absolute value) in percent on the estimated NO_x emissions and the NO_2 lifetime for the three selected urban areas in 2019 for each source of uncertainty and given by category (wind data, TROPOMI data, fit parameters and location of the source). The overall uncertainty is calculated as: $\sum_i \sqrt{\frac{RD_i^2}{x_i^2}}$, with RD the relative difference and x the magnitude of change applied for each test

Uncertainty source	Change applied	City	Impact on estimated NO_x emissions (%)	Impact on estimated NO_2 lifetime (%)
Wind data				
Wind direction	Increased by 5%	London	10.93	03.03
		Manchester	02.12	02.16
		Birmingham	04.71	18.75
Wind speed	Increased by 5%	London	02.53	05.17
		Manchester	03.92	05.84
		Birmingham	01.09	03.99
TROPOMI data				
NO_2 tropospheric column	Increased by 50%	London	50.00	2×10^{-4}
		Manchester	50.00	9×10^{-5}
		Birmingham	50.00	3×10^{-4}
Fit parameters				
σ	Decreased by 1/3 (from 15 km to 10 km)	London	2×10^{-4}	2×10^{-5}
		Manchester	3×10^{-3}	10^{-3}
		Birmingham	00.01	00.01
λ	Decreased by 50% (from 1/3 to 1/6)	London	3×10^{-3}	3×10^{-4}
		Manchester	8×10^{-3}	4×10^{-3}
		Birmingham	10^{-3}	10^{-3}
A	Increased by 15%	London	5×10^{-4}	5×10^{-5}
		Manchester	3×10^{-5}	2×10^{-5}
		Birmingham	5×10^{-5}	8×10^{-5}
B	Increased by 15%	London	2×10^{-7}	4×10^{-7}
		Manchester	8×10^{-7}	4×10^{-7}
		Birmingham	9×10^{-7}	5×10^{-7}
Overall (for the uncertainties on the wind data, TROPOMI data and the fit parameters)				
		London	2.46	1.20
		Manchester	1.34	1.25
		Birmingham	1.39	3.83
Location of the source				
Location of the centre of the source in the 1 km grid	+0.25 km in the x and y axis (Fig. S2)	London	00.21	00.22
		Manchester	00.04	00.95
		Birmingham	01.02	00.56
Location of the centre of the source	+5 km	London	01.89	01.81
		Manchester	05.98	21.29
		Birmingham	26.42	29.98

a similar NO_x emission has been found in their work for London (~115 kT). Pope *et al.* (2022)[17] also found larger differences in the NAEI NO_x emissions with at least an overestimation of 55% in London, reaching 105% in Manchester (Fig. 4).

While the NO_2 lifetime in Birmingham is similar in both studies, the lifetime in London calculated in this study is twice lower than the one in Pope *et al.* (2022)[17] and almost five times lower in Manchester.

4.3 Sensitivity test

There are several potential sources of error that need to be considered when the NO_x emissions and the NO_2 lifetime are estimated. These sources of error have been categorised as related to the location of the center of our source, the information given by the wind fields (direction and speed), the value of the NO_2 tropospheric column and the fit parameters. Indeed, the fitting procedure is based on the use of *a priori* plume spread (σ), NO_2 decay rate (λ), emission enhancement (A) and the background NO_2 (B), and thus the results may depend on their selection.

All the tested values and their impact on the estimated NO_x emissions and NO_2 lifetime are summarised in Table 1. It is clear that the calculated NO_x emissions vary linearly with the NO_2 tropospheric column values. By increasing the value of these columns by 50%, the NO_x emissions are also increased by 50%, but it is worth noting it does not impact the calculated NO_2 lifetime. It is also worth reminding that the validation studies show biases in the NO_2 tropospheric columns which

differ between the background and enhanced conditions. Even if the performed test does not represent the reality of the measured conditions (since the source of uncertainties is multiple and varies according to the NO_2 levels, and so a test should be applied for each source of uncertainty and the different NO_2 conditions), the use of this constant large bias represents a worst-case scenario.

Otherwise, the main source of uncertainty in the calculation is in the wind data. By artificially changing the wind direction, or the wind speed, it can influence the calculated emissions and lifetimes. In these tests, the wind direction largely impacts the NO_x emission in London (11%), while it mainly impacts the NO_2 lifetime in Birmingham (19%). The wind speed has a more limited impact on the results.

These tests also show that the initial conditions of the fit parameters (σ, λ, A and B) have negligible impact on the estimates as shown in other studies.[13]

Adding in quadrature for the uncertainties is commonly used to estimate the overall uncertainty.[5,20,37] It is worth noting that each uncertainty tested in Table 1 only represents a "snapshot" of the response for the selected test with the selected magnitude. These tests fairly highlight the main source of uncertainties, but a complete picture can only be obtained by performing several tests, *i.e.* using several perturbation factors for each source of uncertainty. Moreover, to have a proper conclusion, these uncertainties need to be weighted by the magnitude of the perturbation which has been used. This weighted sum has been calculated (for the wind fields, the NO_2 tropospheric column and the fit parameters) and presented in the category "overall". This also assumes that each uncertainty is independent as done for the evaluation of the uncertainties in previous studies.[5,20,37] This results in a low overall uncertainty in emissions (<3%) and lifetime (<4%).

The calculations of the emissions and lifetimes are based on the assumption that each source is well centred within a 1 km × 1 km grid cell. Thus, the coordinates have been changed but kept within the initially selected 1 km^2 grid cell. Instead of defining the centre of the source as the centroid of the selected NAEI grid cell, the coordinates of this centre have been slightly moved by 0.25 km in the x and y axis as shown in Fig. S2.† This test allows keeping the same NAEI area as the initial estimate and has a minor impact. However, by applying a larger offset (+5 km), it has been shown that the location of the centre of the source has a larger impact, up to 26% in the NO_x emission and 30% in the NO_2 lifetime in Birmingham. Even if these values are high compared to the variation of the NAEI NO_x emission related to this change of area (0.19% for London, 2.97% for Manchester, and 0.71% for Birmingham), the large impact of this later test as seen in Birmingham needs to be qualified. Indeed, a shift of 5 km of the centre of the source in Birmingham corresponds to 50% of its estimated plume spread (Section 4.1).

4.4 Weekday–weekend and seasonal NO_x emissions and mean NO_2 lifetime

The TROPOMI data have been split into weekdays and weekends to estimate the weekly cycle in the NO_x emission and the NO_2 lifetime. The calculations corresponding to the weekday data and the weekend data have been done separately. The standard deviation of the estimates shows the results for the pressure levels from 1000 to 925 hPa, and from 1000 to 875 hPa, as done for the annual estimates.

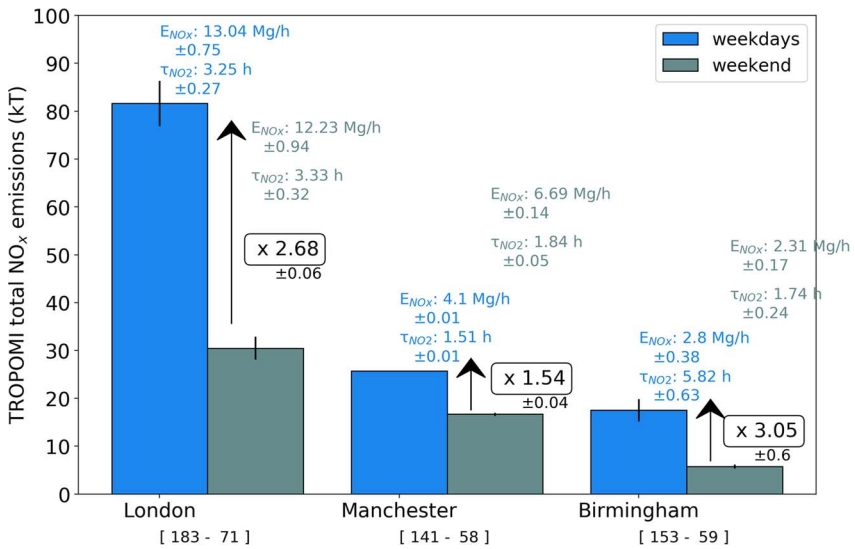

Fig. 5 TROPOMI NO_x emission (in kT) in 2019 split by weekdays (blue) and weekends (green) for London, Manchester and Birmingham, using the vertically integrated 1000–900 hPa wind field. The mean NO_x emission rates (in Mg h^{-1}) and mean TROPOMI NO_2 lifetime (in h) with their standard deviation are also provided above the corresponding bars. The black arrows with the framed black numbers highlight the ratio of NO_x emission between weekends and weekdays. The black vertical line for each bar corresponds to the standard deviation of the TROPOMI NO_x emission. These standard deviations are calculated using also the estimates based on vertically integrated wind fields between 1000 and 925 hPa, and between 1000 and 875 hPa. The number of days of observations used for the calculations of the mean emission rate and lifetime is provided below each corresponding bar in square brackets.

Fig. 5 shows the weekday total NO_x emissions are larger than the weekend emissions, by a factor of 1.54 (±0.04) for Manchester, 2.68 (±0.06) for London and 3.05 (±0.6) for Birmingham. However, there is no drastic difference in the mean NO_x emission rate calculated for London and Birmingham between weekdays and weekends, with ∼13 Mg h^{-1} (±0.75) and ∼12.2 Mg h^{-1} (±0.94), respectively for London, and with ∼2.8 Mg h^{-1} (±0.38) and ∼2.3 Mg h^{-1} (±0.17) respectively for Birmingham. It can be also seen that the weekday–weekend emission rates in London are similar to its annual value (Fig. 3). It is worth noting that the mean NO_x emission rate in Manchester is larger during the weekend (∼6.7 Mg h^{-1} ± 0.14) than during the weekdays (∼4.1 Mg h^{-1} ± 0.01). A larger difference in the NO_2 lifetime is calculated for Birmingham, with a mean value close to 6 h during the weekdays, while it is close to 2 h during the weekend. This difference in lifetime in Birmingham is similar to its ratio of emissions in weekdays *versus* weekends.

A larger NO_2 mean emission rate for weekdays and for the weekends is found for London. This leads to larger NO_x total emissions in both cases compared to the two other cities.

A similar separation has been done by season defined as winter (December–January–February: DJF), spring (March–April–May: MAM), summer (June–July–August: JJA), and autumn (September–October–November: SON). While the annual and the weekly estimates use observations for all months, it has been found that the fitting procedure using observations split by seasons does not work in all cases. The most favourable seasons to estimate the emissions depend on the selected city. Spring and summer are the most favourable seasons in Birmingham, summer and autumn for the Manchester area, and spring–summer–autumn for London. The seasonal impact on the estimates is shown in Fig. 6.

These more favourable seasons are characterised by a larger SNR in Birmingham and Manchester, even if in Manchester, autumn (SON) does present a large difference in SNR with spring (MAM) (Fig. S3†). In London, the summer and autumn are also characterized by a larger SNR which matches with the possibility to infer the NO_x emissions. However, even high, spring (MAM) has a lower SNR compared to winter (DJF). Winter is characterized by a larger mean wind speed (∼30 km h^{-1}) for the cities (Fig. S4†). This might suggest that the favourable conditions to infer the seasonal NO_x emission are a combination of a high SNR and low wind speed. The influence of the wind speed is not surprising since it has been highlighted in the sensitivity test in Table 1. Moreover, a lower wind speed might contribute to reducing the dilution of NO_2 and so large columns can remain over the source region and increase the SNR. Interestingly, there is no dramatic bias in the number of days per season used to estimate the emissions for the three urbanised areas (Fig. S5†), even if January is the month with less days of available observations (not shown).

Fig. 6 shows the larger NO_x emissions and mean emission rates that are calculated in London for the 3 seasons (MAM, JJA and SON), reaching up to 27 kT (±3) in autumn. London does not show a large change in the seasonal NO_2 lifetime. In comparison, Manchester presents a mean NO_2 lifetime almost 4 times larger in summer (6.13 h ± 0.38) than in autumn (1.64 h ± 0.02), which is surprising since most of the mid-latitude cities are characterised by lower NO_2 lifetime in summer.[8,40] The analysis of the temperature at 2 m, precipitations and solar radiation do not explain this larger summer lifetime. There is also no drastic change in the mean NO_2 tropospheric column in summer (∼3 × 10^{15} molecules per cm^2) compared to autumn (∼4 × 10^{15} molecules per cm^2) in Manchester (not shown). A different chemical regime might explain the large difference in the lifetime calculated between both seasons. It is also worth noting that Birmingham has a larger mean NO_x emission rate in summer (2.25 Mg h^{-1} ± 0.15) than Manchester (1.32 Mg h^{-1} ± 0.06). The summer NO_x emission is also the lower seasonal emission for Manchester (∼3 kT ± 0.14 compared to its ∼10 kT ± 0.28 autumn emission) and for Birmingham (∼5 kT ± 0.34 compared to its ∼8.5 kT ± 0.47 spring emission). The road

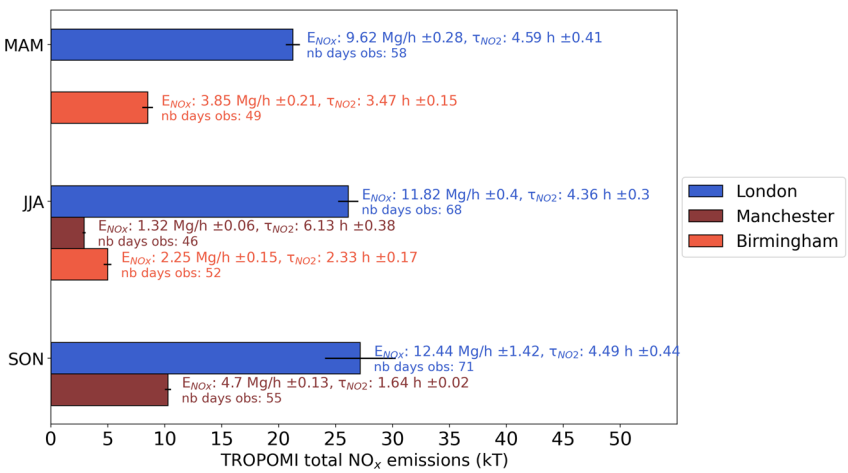

Fig. 6 Seasonal TROPOMI total NO_x emission (in kT) for London, Manchester and Birmingham. Only MAM, JJA and SON are represented. The corresponding mean NO_x emission rates (in Mg h^{-1}), mean TROPOMI NO_2 lifetime (in h) and the number of days of observations used for the calculations of these mean values are also provided. The black vertical line for each bar corresponds to the standard deviation of the TROPOMI NO_x emission. All standard deviations are calculated using also the estimates based on vertically integrated wind fields between 1000 and 925 hPa, and between 1000 and 875 hPa.

transport accounts for around 47% and 50% of the NAEI total NO_x emission respectively for both urban areas, thus these lower summer NO_x emissions might be related to a reduction in the traffic during this period in Manchester and Birmingham. However, this assumption needs to be further studied and remains speculative without a proper sectoral analysis and a detailed analysis of the atmospheric chemical composition.

These results on the temporal variation might suggest the implementation of different mitigation strategies on NO_2 pollution for these cities. In London, the policies could target the weekday emissions for all seasons. Birmingham might also tackle its weekday emissions for both seasons, spring and summer (where the calculation has been done). On the other hand, Manchester could benefit from an improved air quality with measures on weekend emissions since the emission rate and the lifetime are larger during the weekends. In Manchester, a seasonal approach can be beneficial to reach different objectives. Targeting the summer emissions in Manchester might help to reduce the number of consecutive hours of exposure to NO_2 exceedance due to the longer NO_2 lifetime, while the reduction of autumnal emissions might decrease the NO_2 concentrations since the mean NO_x emission rate is higher.

5. Conclusions

By combining satellite NO_2 measurements from the TROPOMI instrument and the wind information from ECWMF, this work has shown the possibility to infer total NO_x emissions and mean NO_2 lifetime over three highly densified urban areas in the UK, namely London, Manchester and Birmingham.

This results in an annual NO_x emission in 2019 of 113 kT ($\pm$6.47) for the 100 km $\times$ 100 km area over London, and 37 kT ($\pm$0.36) and 22 kT ($\pm$2.62) for the 60 km $\times$ 60 km area over Manchester and Birmingham, respectively. In comparison with the NAEI, these estimates are 6% and 18% higher for Manchester and London, respectively, and 33% lower for Birmingham. This remains in fair agreement with the UK national inventory, especially considering that Pope *et al.* (2022)[17] found larger discrepancies with the same inventory (from 55% to 105%).

Sensitivity tests have been undertaken on the calculations and show that the main source of uncertainty in the calculation of the annual NO_x emission and mean NO_2 lifetime is the wind data if we exclude the uncertainty in the NO_2 measurements themself. Indeed, a variation of 5% in the wind direction can lead to a change in the annual NO_x total emission close to 11% over London and a change around 19% of the annual mean NO_2 lifetime in Birmingham.

This works also shows the possibility to infer the temporal variation, *i.e.* for weekends and weekdays, and the seasonal cycle under certain conditions. It has been shown that the seasonal estimates require a large SNR and low wind speed which are not found in winter in the studied cases. This potentially shows if the emissions decrease in future years, the estimation of NO_x emissions with the TROPOMI measurements might be more challenging due to a reduced SNR.

The study shows that the weekday total NO_x emissions are larger than emissions in the weekend, by a factor of 1.54 ($\pm$0.04) for Manchester, 2.68 ($\pm$0.06) for London and 3.05 ($\pm$0.6) for Birmingham. However, Manchester has a larger NO_x mean emission rate during the weekend ($\sim$6.7 Mg h^{-1} $\pm$ 0.14) than during the weekdays ($\sim$4.1 Mg h^{-1} $\pm$ 0.01). Birmingham has a longer NO_2 mean lifetime in weekdays ($\sim$6 h $\pm$ 0.63) than in the weekends ($\sim$2 h $\pm$ 0.24).

London presents similar mean NO_x emission rates for 3 seasons (spring, summer and autumn) ranging from 10 to 12 Mg h^{-1}, and NO_2 lifetime, near 4 h. In comparison, Manchester presents a mean NO_2 lifetime almost 4 times larger in summer (6.13 h $\pm$ 0.38) than in autumn (1.64 h $\pm$ 0.02). It is also worth noting that Birmingham has a larger mean NO_x emission rate in summer (2.25 Mg h^{-1} $\pm$ 0.15) than Manchester (1.32 Mg h^{-1} $\pm$ 0.06).

The findings suggest that the mitigation of NO_2 concentrations in Manchester could require a different emission management strategy than in London and Birmingham. Perhaps the policies in Manchester could be focussed in a targeted manner on reducing weekend emissions (where both emission rate and NO_2 lifetime are longest), whereas in London and Birmingham a more weekday focussed approach can be required as there is less seasonal variation and weekday emissions are much greater than weekend emissions.

The analysis also highlights potential sources of improvement in the method. The information provided by the wind data is critical and can be further investigated, by testing another source of data (*e.g.* using data from the National Centers for Environmental Prediction – NCEP) or using more spatially resolved wind fields such as those calculated by the Weather Research and Forecasting (WRF) model, or by taking into account the temporal variations in wind fields.[27] In addition, the calculation of the satellite-based NO_x emission relies on a prescribed NO_x/NO_2 ratio which might be refined by converting the tropospheric NO_2 columns for each pixel into tropospheric NO_x columns prior to the fitting procedure. The results can also be refined by using the algorithm designed for multi-sources, isolating the impact of surrounding sources in the case of clusters of area sources which can be relevant for most of the conurbations in the UK, and estimating the industrial, urban, and background contributions.[13] Finally, the use of new geostationary measurements with the scheduled Sentinel-4 mission will also help to investigate the impact of the diurnal variability of NO_2 in the estimates.

Data availability

The ERA-5 wind data are freely available at **https://cds.climate.copernicus.eu/cdsapp#!/dataset/reanalysis-era5-pressure-levels?tab=overview**. The ERA-5 PBL, total precipitation, the temperature at 2 m and surface net solar radiation data are available at **https://cds.climate.copernicus.eu/cdsapp#!/dataset/reanalysis-era5-single-levels?tab=form**. The offline TROPOMI NO_2 columns are publicly available on **https://s5phub.copernicus.eu**. The NAEI emission data are publicly available at **https://naei.beis.gov.uk/data/**.

Conflicts of interest

There are no conflicts to declare.

Acknowledgements

The author would like to thank Enrico Dammers (TNO) for his fruitful discussion on the EMG fitting function, Marco Pizzolato (Ricardo Energy and Environment) for the preparation of the NAEI NO_x emission file used for this work and Scott Hamilton (Ricardo Energy and Environment) for his useful comments on the manuscript.

References

1 J. H. Seinfeld and S. N. Pandis, *Atmospheric Chemistry and Physics: from Air Pollution to Climate Change*, 2nd edn, John Wiley and Sons, New York, 2006, pp. 204–275.
2 COMEAP, *Associations of Long-term Term Average Concentrations of Nitrogen Dioxide with Mortality – A Report by the Committee on the Medical Effects of Air Pollutants*, 2018.
3 Defra, *RoTAP: Review of Transboundary Air Pollution: Acidification, Eutrophication, Ground Level Ozone and Heavy Metals in the UK*, 2012.
4 M. Crippa, D. Guizzardi, M. Muntean, E. Schaaf, F. Dentener, J. A. van Aardenne, S. Monni, U. Doering, J. G. J. Olivier, V. Pagliari and G. Janssens-Maenhout, Gridded emissions of air pollutants for the period 1970–2012 within EDGAR v4.3.2, *Earth Syst. Sci. Data*, 2018, **10**, 1987–2013.
5 S. Beirle, K. F. Boersma, U. Platt, M. G. Lawrence and T. Wagner, Megacity Emissions and Lifetimes of Nitrogen Oxides Probed from Space, *Science*, 2011, 1737–1739.
6 Z. Lu, D. G. Streets, B. de Foy, L. N. Lamsal, B. N. Duncan and J. Xing, Emissions of nitrogen oxides from US urban areas: estimation from Ozone Monitoring Instrument retrievals for 2005–2014, *Atmos. Chem. Phys.*, 2015, **15**, 10367–10383.
7 B. N. Duncan, L. N. Lamsal, A. M. Thompson, Y. Yoshida, Z. Lu, D. G. Streets, M. M. Hurwitz and K. E. Pickering, A space-based, high-resolution view of notable changes in urban NO_x pollution around the world (2005–2014), *J. Geophys. Res.*, 2016, **121**, 976–996.
8 K. Lange, A. Richter and J. P. Burrows, Variability of nitrogen oxide emission fluxes and lifetimes estimated from Sentinel-5P TROPOMI observations, *Atmos. Chem. Phys.*, 2022, **22**, 2745–2767.
9 J. P. P. Veefkind, I. Aben, K. McMullan, H. Förster, J. de Vries, G. Otter, J. Claas, H. J. J. Eskes, J. F. F. de Haan, Q. Kleipool, M. van Weele, O. Hasekamp, R. Hoogeveen, J. Landgraf, R. Snel, P. Tol, P. Ingmann, R. Voors, B. Kruizinga, R. Vink, H. Visser and P. F. Levelt, TROPOMI on the ESA Sentinel-5 Precursor: A GMES mission for global observations of the atmospheric composition for climate, air quality and ozone layer applications, *Remote Sens. Environ.*, 2012, **120**, 70–83.
10 P. F. Levelt, J. Joiner, J. Tamminen, J. P. Veefkind, P. K. Bhartia, D. C. Stein Zweers, B. N. Duncan, D. G. Streets, H. Eskes, R. van der A, C. McLinden, V. Fioletov, S. Carn, J. de Laat, M. deLand, S. Marchenko, R. McPeters, J. Ziemke, D. Fu, X. Liu, K. Pickering, A. Apituley, G. González Abad, A. Arola, F. Boersma, C. Chan Miller, K. Chance, M. de Graaf, J. Hakkarainen, S. Hassinen, I. Ialongo, Q. Kleipool, N. Krotkov, C. Li, L. Lamsal, P. Newman, C. Nowlan, R. Suleiman, L. G. Tilstra, O. Torres, H. Wang and K. Wargan, The Ozone Monitoring Instrument: overview of 14 years in space, *Atmos. Chem. Phys.*, 2018, **18**, 5699–5745.
11 W. H. Organization, *WHO Global Air Quality Guidelines: Particulate Matter ($PM_{2.5}$ and PM_{10}), Ozone, Nitrogen Dioxide, Sulfur Dioxide and Carbon Monoxide*, 2021.
12 D. M. Brookes, J. R. Stedman, A. J. Kent, S. L. Whiting, R. A. Rose, C. J. Williams, K. L. Pugsley, J. V. Wareham and A. Pepler, Technical report on UK supplementary assessment under The Air Quality Directive (2008/50/EC), *The Air Quality Framework Directive (96/62/EC) and Fourth Daughter Directive (2004/107/EC) for 2019*, 2021.
13 V. Fioletov, C. A. McLinden, D. Griffin, N. Krotkov, F. Liu and H. Eskes, Quantifying urban, industrial, and background changes in NO_2 during the COVID-19 lockdown period based on TROPOMI satellite observations, *Atmos. Chem. Phys.*, 2022, **22**, 4201–4236.
14 B. Mijling and R. J. van der A, Using daily satellite observations to estimate emissions of short-lived airpollutants on a mesoscopic scale, *J. Geophys. Res.*, 2012, **117**, D17.
15 A. Lorente, K. F. Boersma, H. J. Eskes, J. P. Veefkind, J. H. G. M. van Geffen, M. B. de Zeeuw, H. A. C. Denier van der Gon, S. Beirle and M. C. Krol, Quantification of nitrogen oxides emissions from build-up of pollution over Paris with TROPOMI, *Sci. Rep.*, 2019, 20033.
16 B. de Foy, J. L. Wilkins, Z. Lu, D. G. Streets and B. N. Duncan, Model evaluation of methods for estimating surface emissions and chemical lifetimes from satellite data, *Atmos. Environ.*, 2014, **98**, 66–77.
17 R. J. Pope, R. Kelly, E. Marais, A. M. Graham, C. Wilson, J. J. Harrison, S. J. A. Moniz, M. Ghalaieny, S. R. Arnold and M. P. Chipperfield, Exploiting satellite measurements to explore uncertainties in UK bottom-up NO_x emission estimates, *Atmos. Chem. Phys.*, 2022, **22**, 4323–4338.
18 M. Pommier, C. A. McLinden and M. Deeter, Relative changes in CO emissions over megacities based on observations from space, *Geophys. Res. Lett.*, 2013, **40**, 3766–3771.
19 L. C. Valin, A. R. Russell and R. C. Cohen, Variations of OH radical in an urban plume inferred from NO_2, *Geophys. Res. Lett.*, 2013, **40**, 1856–1860.
20 V. Fioletov, C. A. McLinden, N. Krotkov and C. Li, Lifetimes and emissions of SO_2 from point sources estimated from OMI, *Geophys. Res. Lett.*, 2015, **42**, 1969–1976.
21 S. Churchill, A. Misra, P. Brown, S. Del Vento, E. Karagianni, T. Murrells, N. Passant, J. Richardson, B. Richmond, H. Smith, R. Stewart, I. Tsagatakis, G. Thistlethwaite, D. Wakeling, C. Walker, J. Wiltshire, M. Hobson, M. Gibbs, T. Misselbrook, U. Dragosits and S. Tomlinson, *UK Informative Inventory Report (1990 to 2019). National Atmospheric Emissions Inventory*, 2021.

22 M. Kendon, M. McCarthy, S. Jevrejeva, A. Matthews, T. Sparks and J. Garforth, State of the UK Climate 2019, *Int. J. Climatol.*, 2020, **40**(S1), 1–69.

23 T. Verhoelst, S. Compernolle, G. Pinardi, J.-C. Lambert, H. J. Eskes, K.-U. Eichmann, A. M. Fjæraa, J. Granville, S. Niemeijer, A. Cede, M. Tiefengraber, F. Hendrick, A. Pazmiño, A. Bias, A. Bazureau, K. F. Boersma, K. Bognar, A. Dehn, S. Donner, A. Elokhov, M. Gebetsberger, F. Goutail, M. Grutter de la Mora, A. Gruzdev, M. Gratsea, G. H. Hansen, H. Irie, N. Jepsen, Y. Kanaya, D. Karagkiozidis, R. Kivi, K. Kreher, P. F. Levelt, C. Liu, M. Müller, M. Navarro Comas, A. J. M. Piters, J.-P. Pommereau, T. Portafaix, C. Prados-Roman, O. Puentedura, R. Querel, J. Remmers, A. Richter, J. Rimmer, C. Rivera Cárdenas, L. Saavedra de Miguel, V. P. Sinyakov, W. Stremme, K. Strong, M. Van Roozendael, J. P. Veefkind, T. Wagner, F. Wittrock, M. Yela González and C. Zehner, Ground-based validation of the Copernicus Sentinel-5P TROPOMI NO_2 measurements with the NDACC ZSL-DOAS, MAX-DOAS and Pandonia global networks, *Atmos. Meas. Tech.*, 2021, **14**, 481–510.

24 T. Vlemmix, H. J. Eskes, A. J. M. Piters, M. Schaap, F. J. Sauter, H. Kelder and P. F. Levelt, MAX-DOAS tropospheric nitrogen dioxide column measurements compared with the Lotos-Euros air quality model, *Atmos. Chem. Phys.*, 2015, **15**, 1313–1330.

25 A.-M. Blechschmidt, J. Arteta, A. Coman, L. Curier, H. Eskes, G. Foret, C. Gielen, F. Hendrick, V. Marécal, F. Meleux, J. Parmentier, E. Peters, G. Pinardi, A. J. M. Piters, M. Plu, A. Richter, A. Segers, M. Sofiev, Á. M. Valdebenito, M. Van Roozendael, J. Vira, T. Vlemmix and J. P. Burrows, Comparison of tropospheric NO_2 columns from MAX-DOAS retrievals and regional air quality model simulations, *Atmos. Chem. Phys.*, 2020, **20**, 2795–2823.

26 H. Hersbach, B. Bell, P. Berrisford, G. Biavati, A. Horányi, J. Muñoz Sabater, J. Nicolas, C. Peubey, R. Radu, I. Rozum, D. Schepers, A. Simmons, C. Soci, D. Dee and J.-N. Thépaut, ERA5 hourly data on pressure levels from 1979 to present. *Copernicus Climate Change Service (C3S) Climate Data Store (CDS)*, 2018.

27 F. Liu, Z. Tao, S. Beirle, J. Joiner, Y. Yoshida, S. J. Smith, K. E. Knowland and T. Wagner, A new method for inferring city emissions and lifetimes of nitrogen oxides from high-resolution nitrogen dioxide observations: a model study, *Atmos. Chem. Phys.*, 2022, **22**, 1333–1349.

28 EMEP/EAA, *EMEP/EEA Air Pollutant Emission Inventory Guidebook*, 2019.

29 V. E. Fioletov, C. A. McLinden, N. Krotkov, M. D. Moran and K. Yang, Estimation of SO_2 emissions using OMI retrievals, *Geophys. Res. Lett.*, 2011, **38**(21), L21811.

30 B. de Foy, Z. Lu, D. G. Streets, L. N. Lamsal and B. N. Duncan, Estimates of power plant NO_x emissions and lifetimes from OMI NO_2 satellite retrievals, *Atmos. Environ.*, 2015, **116**, 1–11.

31 E. Dammers, C. A. McLinden, D. Griffin, M. W. Shephard, S. Van Der Graaf, E. Lutsch, M. Schaap, Y. Gainairu-Matz, V. Fioletov, M. Van Damme, S. Whitburn, L. Clarisse, K. Cady-Pereira, C. Clerbaux, P.-F. Coheur and J. W. Erisman, NH_3 emissions from large point sources derived from CrIS and IASI satellite observations, *Atmos. Chem. Phys.*, 2019, **19**, 12261–122939.

32 E. Jones, T. Oliphant and P. Peterson, *SciPy: Open Source Scientific Tools for Python*, 2001, online available: **http://www.scipy.org/**.

33 I. Ialongo, N. Stepanova, J. Hakkarainen, H. Virta and D. Gritsenko, Satellite-based estimates of nitrogen oxide and methane emissions from gas flaring and oil production activities in Sakha Republic, Russia, *Atmos. Environ.*, 2021, **11**, 100114.

34 D. L. Goldberg, Z. Lu, D. G. Streets, B. de Foy, D. Griffin, C. A. McLinden, L. N. Lamsal, N. A. Krotkov and H. Eskes, Enhanced Capabilities of TROPOMI NO_2: Estimating NO_X from North American Cities and Power Plants, *Environ. Sci. Technol.*, 2019, **53**, 12594–12601.

35 W. W. Verstraeten, K. F. Boersma, J. Douros, J. E. Williams, H. Eskes, F. Liu, S. Beirle and A. Delcloo, Top-down NO_x emissions of European cities based on the downwind plume of modelled, *Sensors*, 2018, **18**, 2893.

36 S. Beirle, C. Borger, S. Dörner, A. Li, Z. Hu, F. Liu, Y. Wang and T. Wagner, Pinpointing nitrogen oxide emissions from space, *Sci. Adv.*, 2019, **5**, 11.

37 C. A. M. Linden, V. Fioletov, M. W. Shephard, N. Krotkov, C. Li, M. V. Martin, M. D. Moran and J. Joiner, Space-based detection of missing sulfur dioxide, *Nat. Geosci.*, 2016, **9**, 496–500.

38 L. C. Valin, A. R. Russell, R. C. Hudman and R. C. Cohen, Effects of model resolution on the interpretation of satellite NO_2 observations, *Atmos. Chem. Phys.*, 2011, 11647–11655.

39 S. Beirle, C. Borger, S. Dörner, H. Eskes, V. Kumar, A. de Laat and T. Wagner, Catalog of NO_x emissions from point sources as derived from the divergence of the NO_2 flux for TROPOMI, *Earth Syst. Sci. Data*, 2021, **13**, 2995–3012.

40 R. V. Martin, D. J. Jacob, K. Chance, T. P. Kurosu, P. I. Palmer and M. J. Evans, Global inventory of nitrogen oxide emissions constrained by space-based observations of NO_2 columns, *J. Geophys. Res.: Atmos.*, 2003, **108**, D17.